ELSEVIER

Agricultural and Forest Meteorology 95 (1999) 67–84

AGRICULTURAL AND FOREST METEOROLOGY

Evapotranspiration model for semi-arid shrub-lands tested against data from SE Spain

F. Domingo[a,*], L. Villagarcía[a], A.J. Brenner[b], J. Puigdefábregas[a]

[a]*Estación Experimental de Zonas Áridas, Consejo Superior de Investigaciones Científicas (C.S.I.C), 04001 Almería, Spain*
[b]*School of Natural Resources and Environment, The University of Michigan 430 E. University, Ann Arbor, MI 48109-1115, USA*

Received 4 August 1998; received in revised form 17 March 1999; accepted 23 March 1999

Abstract

A model was developed that predicted evaporation based on combined information on the physiology of overstorey and substrate, micrometeorological conditions and spatial distribution of plants. Predicted evapotranspiration was verified at stand level for *Retama sphaerocarpa* shrubs, and model parameters were tested to determine their importance in controlling evaporation. Model predictions were compared with evapotranspiration, measured by a Bowen Ratio Energy Balance system (BREB), and transpiration, measured by sap flow of the stems of the shrubs in south eastern Spain. Modifications made to the original two source clumped model in the tested model significantly improved agreement between predicted surface evapotranspiration rates and rates measured by the Bowen Ratio method. The modifications made to the model were improved parameterisation of soil surface conductance, a more detailed description of the radiation balance, and improved parameterisation of the soil aerodynamic conductance terms. Improvements in the soil surface conductance estimates made the most significant change to model predictions, the second two modifications showed no significant improvement in prediction of evapotranspiration. A sensitivity analysis indicated that relatively large variations of leaf area index or albedo caused little variation in evapotranspiration during the period measured, whereas variations in soil water content caused large changes in predicted evapotranspiration. Transpiration rates of shrubs (measured and modelled) indicated an independence from surface soil moisture (0–25 cm) supporting the view that *R. sphaerocarpa* had access to reserves of water deep in the soil which enabled it to survive and grow vigorously in this type of semiarid environment. Thus, it was concluded that land use changes which affect redistribution of water resources (overland and subsurface flow) may threaten the stability survival of *R. sphaerocarpa* stands.

Keywords: *Retama sphaerocarpa*; Evapotranspiration; Soil evaporation; Transpiration; Clumped; Modelling

1. Introduction

Evapotranspiration is the combination of evaporation from soil and transpiration from vegetation. Its calculation is central to the analysis of water balances of both naturally vegetated and agricultural lands. Mathematical modelling of evapotranspiration is an important tool since measurements of evaporation are difficult and costly to obtain. Measurements give information that is local in time and space, whereas answers to many of the important questions require estimates over large catchment areas, and long time scales. Southeastern Spain is undergoing rapid

*Corresponding author. Tel.: +34-950-27-64-00; fax: +34-950-27-71-00; e-mail: poveda@eeza.csic.es

0168-1923/99/$ – see front matter
PII: S0168-1923(99)00031-3

changes in land use, dryland farming is becoming less viable and current agricultural activities focus increasingly on irrigation. There are also proposals to plant forests for pulpwood production on the slopes of local mountain ranges (Sierras). The impact of this type of vegetation change on the hydrologic balance is unclear for the slopes on which these trees are planted, the species that rely on runoff into the dry river valleys (Ramblas) as well as the recharge of acquifers. To evaluate these potential impacts scientifically, it is necessary to quantify water use in the current ecosystem.

Among the many evaporation models that have been developed, mainly for agricultural crops, the best known is the unilayer or single-source Penman–Monteith evaporation model (Monteith, 1965) which has been applied successfully to crops and canopies over the last 30 years. This model assumes that canopies can be regarded as a single uniform surface or 'big-leaf'. Semiarid lands, characterised by patches of vegetation and open spaces, do not satisfy the big-leaf assumption as sources/sinks of fluxes may occur at significantly separated canopy and soil surfaces. Hence, the single-layer Penman–Monteith model has been extended to two or more layers (Shuttleworth and Wallace, 1985; Choudhury and Monteith, 1988; Shuttleworth and Gurney, 1990). The model explicitly specifies energy exchanges at canopy and soil leading to improved predictions of evaporation from sparsely vegetated surfaces (Rouse et al., 1992; Nichols, 1992). Although these two source models account for evaporation from both plant and soil (evapotranspiration) they still assume a uniform canopy coverage. Brenner and Incoll (1997) extended the approach of Dolman (1993) by dividing the surface into vegetated and non-vegetated components, and allowed the substrate that existed underneath the overstory to act as a distinct evaporation source. Brenner and Incoll (1997) showed that this improved estimates of plant evaporation when compared to the Shuttleworth and Gurney formulation. The adaptation of the combination equation of Penman–Monteith to sparse clumped vegetation should provide an improvement in the understanding of the annual use of water by the vegetation components that exist in semi-arid environments.

This paper presents the results obtained in a series of experiments aimed at parameterising and validating the multi-layer evapotranspiration model developed by Brenner and Incoll (1997) for a sparse clumped *Retama sphaerocarpa* stand at the Rambla Honda Field Site (Tabernas, Almería, Spain). The model combines information on the physiology of the overstorey (perennials) and the substrate (soil, annuals), as well as information on the spatial distribution of vegetation clumps and micrometeorological data. Predicted evapotranspiration is compared with measured values from a Bowen Ratio energy balance (BREB) system and predicted plant transpiration with sap flow in the *R. sphaerocarpa* shrubs. A sensitivity analysis of the model is also presented.

This study formed part of a broader project on the estimation of surface evaporation in semi-arid environments using models developed for plant communities with different canopy structures. The project will ultimately combine these models with distributed information of land cover to estimate evapotranspiration at the level of whole catchments with heterogeneous surfaces (vegetated and non-vegetated). This tool will further the study of the impact of climate and land use change scenarios on evaporation and catchment water balance.

2. Theory

The evapotranspiration model on which this study is based was developed by Brenner and Incoll (1997), and was called the 'clumped' model, and will here be referred to as the 'original' model. The 'original' model was derived from combining the approaches of the sparse-crop model of Shuttleworth and Wallace (1985), where vegetation is assumed to be uniformly distributed over a surface, and that of Dolman (1993) where energy was partitioned between bush and bare soil based on their respective fractional covers. The 'original' model differed from Dolman's in that the evaporation could occur from the substrate (soil) both under the overstorey (shrub) and in the open. Parallel energy balances were calculated, for shrub, soil under shrub and bare soil (see Brenner and Incoll (1997) for a full description and derivation). This paper describes modifications to the 'original' model which were made as a result of new field measurements. These modifications concerned the following model components:

2.1. Calculation of net radiation absorbed by R. sphaerocarpa, understorey and soil

In sparse vegetation it is unlikely that the radiation balance is horizontally uniform across the surface. This heterogeneity needs to be considered when both measuring and modelling radiation absorbed by plants and soil. It is known that plants and soil have different emissive and reflective properties, and it is necessary to evaluate the importance of these differences in terms of both overall surface energy balance and the energy balance of each component. A schematic diagram of the energy balance of the system is shown in the Fig. 1.

We will represent radiative fluxes (R) and soil heat fluxes (G) with the following notation. For radiative fluxes, the first subscript denotes the type of radiation, s for shortwave, l for longwave and n for net. The second subscript denotes the source, t for the whole surface (total), a for atmosphere, p for plant, s for soil under shrub (substrate) and bs for bare soil. The third subscript signifies the direction of the flux, u for upward and d for downward. G_s represents the soil heat flux below the understorey and G_{bs} that of the bare soil.

A simple energy partitioning model for sparse vegetation, based on the fractional vegetative area and radiative properties of the surface components

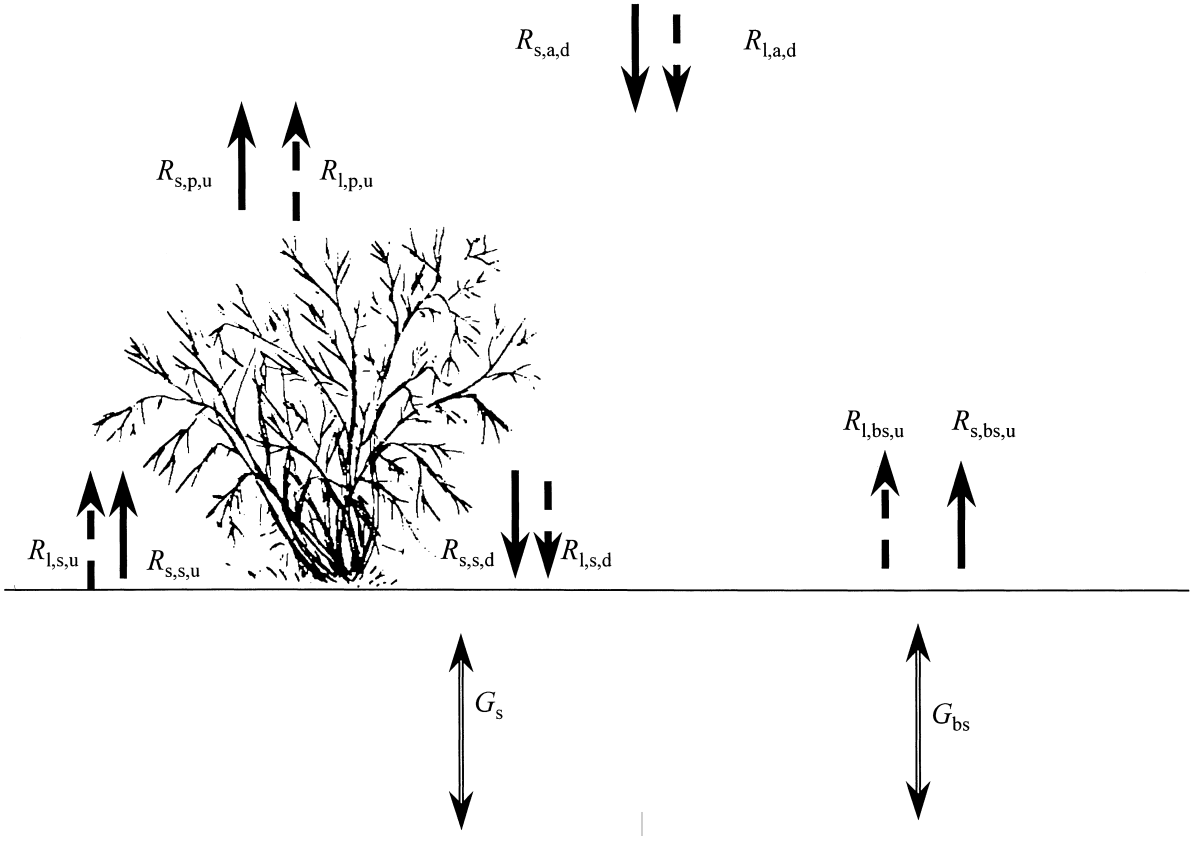

Fig. 1. A simplified schematic diagram of energy flows within sparse vegetation. Shortwave fluxes are represented by solid arrows, longwave fluxes by dashed arrows, and soil heat flux by the unfilled arrows. R represents radiative fluxes and G, soil heat fluxes. For radiative fluxes, the first subscript denotes the type of radiation, s for shortwave and, l for longwave. The second subscript denotes the source, a for atomsphere p for plant, s for soil under shrub (substrate) and bs for bare soil. The third subscript signifies the direction of the flux, u for upward, and d for downward. G_s represents the heat flux below the understorey and G_{bs} that of the bare soil.

(Domingo et al., 1999), was introduced in the 'original' evapotranspiration model. In this, the net radiation for the whole surface ($R_{n,t}$) is partitioned into two components, the net radiation over the vegetated area (in this case *R. sphaerocarpa* and its individual understorey) ($R_{n,p}$) and the net radiation over the bare soil ($R_{n,bs}$) as follows:

$$R_{n,t} = fR_{n,p} + (1-f)R_{n,bs} \quad (1)$$

where f is the fractional vegetation cover. Defining $\delta = R_{n,p} - R_{n,bs}$ leads to

$$\delta = [R_{s,a}(1-\alpha_p) + R_{l,a,d} - R_{l,p,u}] - [R_{s,a}(1-\alpha_{bs}) + R_{l,a,d} - R_{l,bs,u}] \quad (2)$$

and thus

$$\delta = R_{s,a}(\alpha_{bs} - \alpha_p) + \sigma(\varepsilon_{bs}T_{bs}^4 - \varepsilon_p T_p^4) \quad (3)$$

where $R_{s,a}$ is solar radiation, α_{bs} and α_p short wave reflection coefficients (albedo) of bare soil and plant, respectively, σ is the Stephan–Boltzmann's constant, ε_{bs} and ε_p emissivity of bare soil and plant and T_{bs} and T_p soil and plant surface temperature, respectively. Therefore, using Eq. (1) and δ, the net radiation above the vegetated part of the surface ($R_{n,p}$) and the bare soil ($R_{n,bs}$) can be expressed as

$$R_{n,p} = R_{n,t} + \delta(1-f) \quad (4)$$

$$R_{n,bs} = R_{n,t} - \delta f \quad (5)$$

respectively. If energy stored in the plant is assumed to be negligible, the net radiation of the soil under *R. sphaerocarpa* equals

$$R_{n,s} = R_{n,p}e^{-\kappa s} \quad (6)$$

where κ is the extinction coefficient for net radiation of the canopy, s is surface area index that can be related to the leaf area index (L). Thus available energy for each component is calculated in the evapotranspiration model as follows:

$$A_p = R_{n,p} - R_{n,s} \quad (7)$$

$$A_s = R_{n,s} - G_s \quad (8)$$

$$A_{bs} = R_{n,bs} - G_{bs} \quad (9)$$

where A_p is energy available to the plant, A_s and A_{bs} are energy available to soil under shrub and bare soil, respectively, G_s and G_{bs} are heat flux to soil under *R. sphaerocarpa* canopy and bare soil, respectively.

2.2. Soil aerodynamic resistance and r_a^s and r_a^{bs} as functions of wind speed

The aerodynamic resistance (r_a^{bs}) between the bare soil surface and air between the clumps at what was considered to be mean surface flow height (z_m), was calculated in the 'original' model between two limits. When the fractional vegetative cover $f = 0$, r_a^{bs} was assumed to equal r_a^b Eq. (10) (for a better understanding, in the following sections we follow the same notation and symbols as in Brenner and Incoll, 1997).

$$r_a^b = \frac{\ln(z_m/z_0')^2}{k^2 u_m} \quad (10)$$

where u_m is the wind speed at z_m, z_0' the roughness length of bare substrate and k the von Karman's constant. When $f = 1$, r_a^{bs} was assumed to equal the aerodynamic resistance for soil under shrub (r_a^s) which was calculated from the equation

$$r_a^s = \left[\frac{he^n}{nK_h}\right][e^{(-nz_0/h)} - e^{(-n(Z_0+d_p)/h)}] \quad (11)$$

where n is eddy diffusivity decay constant, K_h the eddy diffusivity at the top of the canopy and is obtained as a function of friction velocity, d_p the displacement height, h the plant height, z_0 the roughness length of the surface and Z_0 the fixed zero flux height taken as $0.13h$. Since the form of the functional relationship of this change was not known, r_a^{bs} was varied linearly between r_a^{bs} and r_a^s as f changed from 0 to 1.

In the present study a simple field method measured heat transport by energy balances on pairs of adjacent sensors, heated and unheated, following the method of McInnes et al. (1994). These data enabled the calculation of aerodynamic resistances for bare soil and soil under shrub in the field. These empirical relationships of soil aerodynamic resistance as a function of wind speed were used in the 'modified' evapotranspiration model.

2.3. Soil surface resistance r_s^{bs} and r_s^s

In the 'original' model bare soil resistances (r_s^{bs}) were calculated from evaporation rates from soil (λE^{bs}) measured using mini-lysimeters and through a Penman–Monteith type equation:

$$\lambda E^{bs} = \frac{\Delta A^{bs} + [(\rho C_p D_0)/r_a^{bs}]}{\Delta + \gamma[(r_a^{bs} + r_s^{bs})/r_a^{bs}]} \quad (12)$$

where bs indicates variables that relate to bare soil, Δ the slope of the vapour pressure versus temperature curve, γ the psychometric constant, A the total energy available for latent and sensible heat loss, ρ the density of the air, C_p the heat capacity of air at constant pressure and D_o the water vapour saturation deficit. For simplicity, it was assumed that r_s^{bs} equalled r_s^s, although this was known to be untrue. The equation run in the model to predict soil surface resistances was a quadratic equation based on time after wetting (t) in days since the last rainstorms >5.0 mm:

$$r_s^{bs} = r_s^s = 6.72t^2 + 39.66t + 66 \quad (13)$$

In the present study, soil surface resistances were calculated from the evaporation rates of continuously-weighed minilysimeters (E) using Eq. (14), in this case for bare soil:

$$E = \frac{[(0.622\rho/P)(e^*_{T_{bs}} - e_0)]}{r_a^{bs} + r_s^{bs}} \quad (14)$$

where P is atmospheric pressure, $e^*_{T_{bs}}$ the saturation vapour pressure of water at measured soil temperature (T_{bs}), e_0 the measured vapour pressure at z_m, ρ the density of the air and r_a^{bs} is calculated soil aerodynamic resistance (see Section 2.2). A similar equation was used for soil under shrub. Relationships between soil resistance and soil water content for bare soil and soil under shrub were also determined and used in the model.

3. Materials and methods

3.1. Site description

The field site is located in the Rambla Honda, a dry valley near Tabernas, Almeria, Spain (37°8′N, 2°22′W, 630 m altitude). A detailed description of the field site has been given by Puigdefábregas et al. (1996). The valley has been abandoned for several decades, and currently has little agricultural activity apart from small-scale sheep herding. The vegetation is now dominated by three perennial species, *R. sphaerocarpa* (L.) Boiss. shrubs over the valley floor, *Stipa tenacissima* L. tussocks on the steep valley sides and *Anthyllis cytisoides* L. shrubs on alluvial fans between the two. The valley bottoms have deep loamy soils that overlay mica schist bedrock. The field site has an average annual rainfall of 220 mm and a dry period from around June to September. This study focused on *R. sphaerocarpa* which is a woody leguminous deciduous shrub, and grows to 4 m tall and 6 m diameter, with cylindrical photosynthetic stems (cladodes). The shrub has an open canopy structure and deep root system which can extract water from depths below 25 m (Haase et al., 1996b). In the location of the experiment *R. sphaerocarpa* covers about 0.30 of the valley bottom.

3.2. Field measurements

3.2.1. Determining parameters for the evapotranspiration model

A representative stand of *R. sphaerocarpa* was selected in the middle of the dry river bed in Rambla Honda. *R. sphaerocarpa* shrubs are distributed randomly with a clumping mean distances between shrubs of between 1.0–2.0 m and extent of open spaces of between 2.7–6.1 m on average (Haase et al., 1996a). Micrometeorological variables were measured at a reference height (z_r) of 5.0 m, and between the canopy clumps at what was considered to be mean surface flow height (z_m), 1.5 m. The average height of the *R. sphaerocarpa* individuals (h) was approximately 2.0 m and the assumed mean surface flow height was therefore $0.75h$ (Brenner and Incoll, 1997). The instrumented site was located within a typical place into the stand, with four shrubs separated by about 2 m. Measurements were taken during the period from March to May 1997, during a cycle of soil water content of the upper soil layer that went from $\theta = 4\% \rightarrow \theta = 15\% \rightarrow \theta = 4\%$. The rainfall during this period was 86.2 mm.

3.2.1.1. Net radiation and its components. In the radiation balance experiment, four net radiometers (Q7, REBS, Seattle, WA, USA) measured net radiation (R_n) from different surfaces. Three of them positioned sufficiently close to the measured surface to assure that just that surface affected the corresponding sensor: the first one at 0.5 m over the top-centre of a *R. sphaerocarpa* canopy (3.5 m of diameter), the second one under the same *R. sphaerocarpa* canopy and 0.3 m above the ground, and the third net radiometer at 0.5 m above bare soil in the open. A fourth net radiometer was positioned close

to the canopy edge at 3 m height from the ground (0.5 m from the top of the shrub) and hence receiving energy from both shrub and bare soil. A photography taken with a fish-eye lens from the same place where the radiometer was positioned revealed that the proportions viewed were approximately 30% of shrub and 70% of bare soil.

Three unidirectional net radiation sensors were constructed from Q7 net radiometers (REBS, Seattle, WA, USA), by filling one dome with plastic steel liquid resin (RS 691-246, RS Components, Corby, UK) embedded with a thermocouple to measure its temperature (0.5 mm diameter, Type T, Omega Engineering, Broughton Astley, UK). The metal surface was painted matt black (RS 496-782, RS Components, Corby, UK) and the outside of the dome was insulated using polystyrene. The three unidirectional sensors measured net radiation where one side — the covered side — could be quantified knowing the temperature of the black body emitting surface. When combined with measurements of solar radiation and albedo, incident longwave radiation ($z = 3$ m), and emitted longwave radiation from vegetation and soil (0.5 m above bare soil and vegetation next to the net radiometers) could be calculated. Reflection coefficients (albedo) were measured by three albedometers (CM11 and CM5, Kipp and Zonen, The Netherlands) also positioned next to the net radiometers: 0.5 m above the canopy, 0.5 m above bare soil and under the canopy. A solarimeter (CM11, Kipp and Zonen) measured total solar radiation. All radiometers and solarimeters were cross-calibrated over a uniform surface for 11 days and their calibration adjusted to the newest factory calibrated radiometer, assumed to have the most correct calibration. Measurements were recorded every 1 s by a data logger (CR10, Campbell Scientific Ltd., Logan, UT, USA) and averaged every twenty minutes.

3.2.1.2. Soil heat flux and soil temperature. The soil heat flux (G) was calculated by adding the measured flux (F) at a fixed depth (in this case 0.08 m) (HFT-3, REBS, Seattle, WA, USA) to the energy stored in the soil layer above the heat flux plates (S). The specific heat of the soil and the change in temperature over the output interval were required to calculate the stored energy.

Variation of average soil temperature was measured by two thermocouples (TCAV, Campbell Scientific Ltd., Logan, UT, USA) positioned at 0.02 and 0.06 m depth above the heat flux plate. The equation used for calculating S was:

$$S = \frac{C_T[1555(837 + 4190\,\theta)]0.08}{\omega} \qquad (15)$$

where C_T is the change in temperature, 1555 the bulk density of the soil (kg m^{-3}), 837 the specific heat of dry soil (J kg$^{-1\circ}$ C^{-1}), θ is gravimetric soil water content (kg H_2O/kg soil), 4190 the specific heat of water (J kg^{-1} °C^{-1}), 0.08 the depth of flux plate in the soil (m) and ω the interval of time between measurements (s).

Four pairs of heat flux plates, with their corresponding soil thermocouples, were buried at 0.5 m intervals from the centre of a *R. sphaerocarpa* individual, this meant that there were two under the canopy and two in the open. Measurements of soil heat fluxes and soil temperatures were recorded every 1 s by a data logger (CR10, Campbell Scientific Ltd., Logan, UT, USA) and averaged every 20 min, from 4 April to 28 May.

3.2.1.3. Soil water content. Measurements of soil water content (θ) were taken with two techniques:

1. Non-continuous measurements were taken just after rainfall at increasing time intervals until the next rain, e.g. 1, 2, 3, 5, 10, 14, ..., d, with time domain reflectometry (TDR) (1502C, Tektronix, USA) probes. Measurements were taken at 0.10, 0.15 and 0.20 m depths positioned in the same locations as the heat flux plates.
2. Continuous measurements with self balanced impedance bridge (SBIB) probes at 0.15 m depth positioned under the plant and bare soil in a similar location as to the other sensors. This soil humidity sensor has been developed in the Estación Experimental de Zonas Áridas (C.S.I.C.) (Almería, Spain) (Vidal, 1994) and calibrated against TDR probes and the gravimetric method measurements in the field and the laboratory experiments for a wide range of soil salinity and soil temperature (Vidal et al., 1996; Puigdefábregas and Sanchez, 1996). The SBIB sensors permit the simultaneous determination of soil moisture as volumetric soil water content, soil temperature and electrical soil conductivity of the soil, and is based on measurements of the complex electrical impedance presented by

two electrodes immersed in the soil which constitutes the dielectric of separation (Vidal, 1994).

In this study, soil water measurements by TDR agreed well with SBIB measurements and thus SBIB measurements were used for both inputs to the model and Bowen Ratio calculations because of the continuous nature of the measurement.

3.2.1.4. Evaporation from soil. Ten small lysimeters (108 mm diameter and 250 mm length) (Daamen et al., 1993) were installed at 1 m intervals from the centre of the selected *R. sphaerocarpa* shrub. Six of them were set up with load cells, four to the north and two to the east (632-742, RS Components, Corby, UK) that were constantly logged to an accuracy of 1 g (every 1 s and averaged every 20 min) (CR10, Campbell Scientific Ltd., Logan, UT, USA). The lysimeters in the two other directions were weighed manually. The lysimeters were filled with soil taken at the same distance from the shrub as the locations where they were measured. This allowed the retention of the original surface (substrate) in the lysimeter. Soil cores were extracted by excavating plastic tubes that had been hammered into the soil. A plastic cap was fitted to the bottom of the tube to retain the soil and prevent drainage. The lysimeter was placed in a hole lined with a slightly larger plastic tube. New cores were extracted every week or after wetting by rain. Gravimetric soil water content was converted to volumetric water content using the measured soil bulk density (1.55×10^3 kg m^{-3}, Puigdefábregas et al., 1996). Lysimeter measurements were taken from 25 April to 4 May 1997.

3.2.1.5. Soil aerodynamic resistance. Aerodynamic resistances for heat transport were determined from energy balances on pairs of adjacent sensors, heated and unheated. The sensors used were constructed following the design of McInnes et al. (1994) and consisted of a pair of polystyrene foam disks of 0.06 m thickness and 0.15 m diameter, one heated at the surface with a thin round heater and the other unheated. Fine-wire copper–constantan thermocouples (0.27 mm diameter, Type T, Omega Engineering, Broughton Astley, UK) were installed to measure temperatures at the surface and 0.01 m beneath the surfaces of the disks. Aerodynamic resistances for heat transport were determined from energy balances on the heated and unheated pairs. Measurements of aerodynamic resistance were taken at four positions, 1, 2, 3 and 4 m from the centre of a *R. sphaerocarpa* individual. Measurements were recorded every 1 s by a data logger (CR10, Campbell Scientific Ltd., Logan, UT, USA) and averaged every 20 min, from 15 April to 11 May.

3.2.1.6. Additional meteorological data. Aspirated humidity sensors (MTH-A1, ITC, Almería, Spain) measured air temperature and air humidity at z_m and z_r. Two-cup anemometers (A100, Vector Instruments, Rhyl, UK) measured the wind speed at z_m and z_r. An additional cup anemometer was installed at 0.5 m height. Wind direction was measured by a wind vane (W200P, Vector Instruments, Rhyl, UK) at z_r. Average cladode temperature was measured by winding 32 thermocouples (0.27 mm diameter, Type T, Omega Engineering, Broughton Astley, UK) around individual cladodes ensuring that they were in thermal equilibrium with the cladodes. For each shrub four sets of thermocouples, each set having eight sensors connected in parallel, were measured. Radiation errors for the thermocouples were studied and not considered to be significant (Brenner and Incoll, 1997). All measurements were recorded every 1 s by a data logger (CR10, Campbell Scientific Ltd., Logan, UT, USA). 20 min averages were calculated for all data. Leaf boundary layer resistance was calculated from measured differences in temperatures between two metallic replica cladodes, one of which was heated with a constant input power (Domingo et al., 1996).

3.2.1.7. Leaf area, extinction coefficient and clumping. Leaf (cladode) area of *R. sphaerocarpa* was estimated from measurements of transmission of direct beam radiation (DEMON, CSIRO, Canberra, Australia) according to the method described in Brenner et al. (1995) for the same species. Average leaf area index (L_a), defined as leaf area of shrub divided by its projected canopy area, was 3.03 ± 0.37 in June 1993, 2.00 ± 0.29 in June 1994 (Brenner and Incoll, 1997). DEMON measurements made over 22 individuals in 1997 gave an L_a of ca. 2.5 ± 0.15. The average fractional cover (f) for the *R. sphaerocarpa* stand, calculated by image analysis of aerial

photographs was 0.30, slightly lower than the 0.34 calculated by Brenner and Incoll (1997). Taking into account the f of the plot and the L_a of the individual plants measured, the leaf area index for the plot (L) was estimated at 0.75. Calculations of extinction coefficients of *R. sphaerocarpa* canopies from measurements by the DEMON (Brenner et al., 1995) showed that the extinction coefficient (κ) can best be described by a vertical leaf angle distribution. For model calculations presented in this paper, κ was fixed at 0.35 which is approximately equal to κ over the part of the day when radiation was maximal (Brenner et al., 1995). It should be noted that κ calculated from measurements by the DEMON is for wavelengths <380 nm and may well differ from a κ for net radiation, although in the sensitivity analysis conducted it is demonstrated that an increase of κ to 0.6 would only introduce a 2% error.

3.2.2. Validation of the evapotranspiration model

3.2.2.1. Sap flow measurements. The heat balance method for measuring sapflow rates was applied to *R. sphaerocarpa* stems for eight non-consecutive days. Sixteen sapflow gauges (Dynagauge, Dynamax Inc., Houston, USA) were installed at different orientations (N, S, W, E) ranging from 25 to 5 mm stem diameters on three *R. sphaerocarpa* individuals. Sap flow velocity measurements (g of $H_2O\ h^{-1}$) were taken every 5 min and averaged every 20 min. After removing the gauges, leaf area of each stem was measured destructively to relate sap flow velocity to leaf area units. An estimation of the transpiration from the *R. sphaerocarpa* stand was achieved averaging the sixteen gauges and the result multiplied by the leaf area index of the stand ($L = 0.75$).

3.2.2.2. Bowen Ratio measurements. A Bowen Ratio energy balance (BREB) system (Campbell Scientific Ltd., Logan, UT, USA) was used for automatic estimation of surface evaporation. In the system, vapour concentration is measured with single mirror dew point hygrometer (Dew-10, General Eastern Corp. Watertown, USA). Air samples from two heights are aspirated and routed to the cooled mirror after passing through mixing volumes. A solenoid valve controlled which input should go to the cooled mirror. The resolution of the dewpoint temperature measurement was $\pm 0.003^{\circ}C$ over a $\pm 35^{\circ}C$ range. Dew-10 accuracy was $\pm 0.5^{\circ}C$ dew point, with a precision of $\pm 0.05^{\circ}C$. A datalogger (21X, Campbell Scientific Ltd.) recorded the output and controlled the valve that switches the air stream through the cooled mirror every 2 min. Dewpoint temperatures were measured every second and vapour pressures were calculated by the datalogger using the equation described by Lowe (1976). The average vapour pressure at each height is calculated every 20 min. Air temperature was measured at two heights with chromel-constantan fine-wire thermocouples (0.003″ diameter junction).

Initially the BREB system was set up to test its operation under field conditions on such type of sparse vegetation. Data collected indicated that the system operated satisfactorily and tests of the fetch requirement and sensor heights were carried out. Then the BREB systems were set up between the clumps of *R. sphaerocarpa* stand with the upper arm of the Bowen system positioned at $z = 5$ m and the lower arm at $z = 3.5$ m, which is over a metre above the height of the shrubs in this area. Measurements of net radiation were taken from the same BREB mast at 5 m height. Evapotranspiration rates were calculated every 20 min. During the experiment, from the 4 April to 28 May, it was possible to take measurements with two Bowen Ratio systems working at the same time for 15 non-consecutive days. When the two Bowen Ratio systems operated at the same time the average difference in total daily evapotranspiration rate between the systems was 7.6% (Table 1). A difference of 10% between Bowen Ratio systems has been considered acceptable by other authors (Nie et al., 1992; Gurney and Sewell, 1997).

All model simulations were run using Borland Pascal for Windows version 7.0.

4. Results and discussion

4.1. Modified terms of the evapotranspiration model

4.1.1. Comparison of calculated and measured net radiation values

Net radiation for each surface was calculated (Eqs. (4) to (6)) using measured values of δ (albedo,

Table 1
Maximum, minimum, average and standard deviations of the differences (%) in total daily evapotranspiration (15 non-consecutive days from 4 April to 28 May) between A: Two Bowen Ratio systems in the same stand; B: Bowen Ratio measurements and predicted values using the 'original' model; C: Bowen Ratio measurements and predictions of 'original' model with radiation balance modifications. D: Bowen Ratio measurements and predictions of 'original' model with soil surface resitance modifications; E: Bowen Ratio measurements and predictions of 'original' model with soil aerodynamic resitance modifications; F: Bowen Ratio measurements and prediction from the 'modified' model. O is original model, EB is energy balance modification, r_s is soil surface resistance modification, r_a is soil aerodynamic resistance modification

	A	B	C	D	E	F
	Bowen–Bowen (%)	Bowen–O (%)	Bowen–(O + EB) (%)	Bowen–(O + r_s) (%)	Bowen—(O + r_a) (%)	Bowen–Modified (%)
Maximum	16.4	36.5	37.5	6.6	36.0	0.4
Minimum	1.3	2.5	4.7	−11.8	5.4	−25.7
Average ($n = 15$)	7.7	21.2	21.7	−5.4	21.4	−9.5
SD ($n = 15$)	4.8	11.4	10.4	5.8	9.8	7.6

emissivity, extinction coefficient, shown in Table 2) and measured values of surface temperature, solar radiation and total net radiation ($R_{n,t}$). A fixed value of albedo for bare soil (α_{bs}) was used. Predicted $R_{n,p}$ (Eq. (4)), $R_{n,bs}$ (Eq. (5)) and $R_{n,s}$ (Eq. (6)) were compared with direct net radiometer measurements. These comparisons showed no significant differences between calculated and measured values of net radiation (alpha value = 0.05), using the F-test to compare variances: $F = 1.0009$, $n = 634$, $p = 0.4957$ for plant surface; $F = 1.0005$, $n = 634$, $p = 0.4977$ for the bare soil and $F = 1.1839$, $n = 82$, $p = 0.2245$ for the substrate. For the case of the substrate, n is smaller because data were filtered for maximum zenith angles to avoid errors of shading by other individual plants.

Total net radiation ($R_{n,t}$) measured at 3.0 m over both shrub and bare soil also showed no significant difference between calculated and measured values ($F = 1.1332$, $n = 634$, $p = 0.57$).

Based on these results we have included the calculated values of net radiation for plant, bare soil and substrate under shrub, derived from total net radiation $R_{n,t}$ in the evapotranspiration model.

Table 2
Values of fractional vegetative cover, leaf area indices and parameter values used to calculate net radiation for bare soil and plant covers

Variable	Value
Reflection coeff. (α_{bs}) (bare soil)	0.20
Reflection coeff. (α_p) (plant)	0.16
Emissivity (ε_{bs}) (bare soil)	0.94
Emissivity (ε_p) (plant)	0.96
Extinction coefficient (κ)	0.35
Fractional vegetative cover (f)	0.30
Average leaf area indes (L_a) (stand)	2.50
Average leaf area indes (L) (stand)	0.75

4.1.2. Soil aerodynamic resistance

Measurements of soil aerodynamic resistance for heat transport under canopies of *R. sphaerocarpa* and over bare soil could be shown to decrease by a power function with increasing wind speed. The data significantly fitted a power equation ($p < 0.05$) (Fig. 2). This agreed with theoretical and empirical observations of forced convection across a heated horizontal plate in a free air stream (Kays and Crawford, 1980) and is similar to the results obtained for a vineyard using the same method (McInnes et al., 1994, 1996). The relationships found for soil aerodynamic resistance and wind speed measured at reference height (u_r) for the heated and unheated sensors located in the bare soil (r_a^{bs}) and under a *R. sphaerocarpa* canopy (r_a^s) were:

$$r_a^{bs} = 73.7u_r^{-0.17}, \quad (r^2 = 0.55,\ n = 227) \qquad (16)$$

$$r_a^s = 97.1u_r^{-0.16}, \quad (r^2 = 0.67,\ n = 118) \qquad (17)$$

The sensors located between these two locations gave intermediate relationships (Domingo et al., unpublished data). For the purpose of this paper it was assumed that these relationships represent r_a^{bs} and r_a^s, respectively, and were included in the evapotranspiration model.

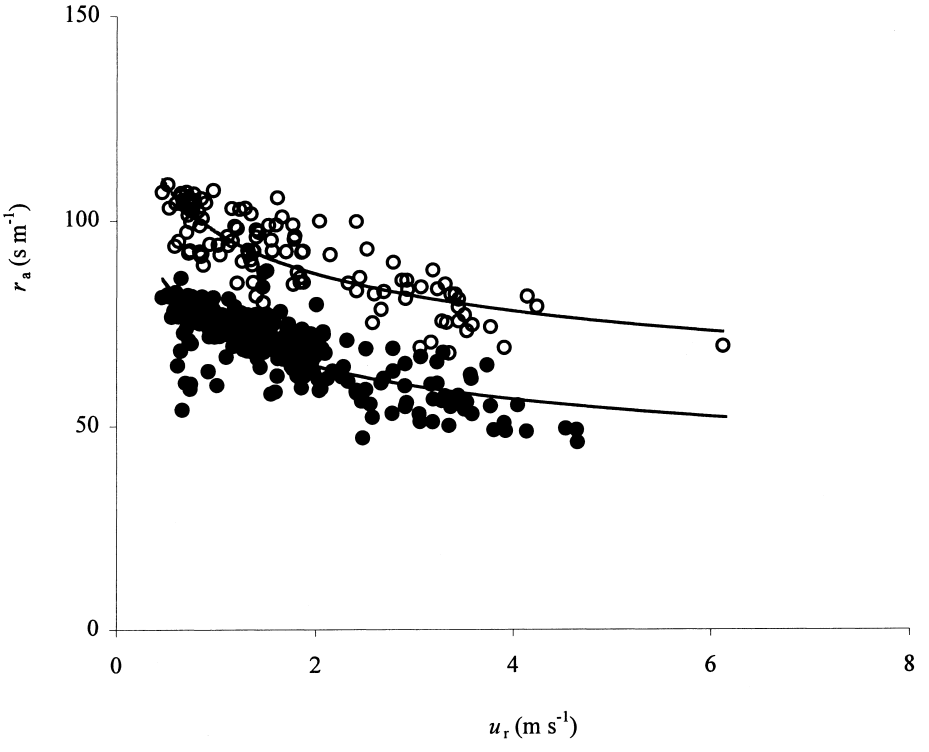

Fig. 2. Relationship between soil aerodynamic resistance and wind speed measured at reference height for bare soil r_a^{bs} (○) and under *R. sphaerocarpa* canopy r_a^s (●). Measurements were recorded every 1 s and averaged every 20 min for the period 15 April to 11 May.

4.1.3. Soil surface resistance

Mass transfer is proportional to a concentration difference, so that for evaporation from a moist surface (E) (Jones, 1992): $E = g_w(\Delta C_w)$, where g_w is the total resistance of the pathway between evaporating sites and the bulk air (soil resistance and soil aerodynamic resistance) and ΔC_w is the water vapour concentration difference between these sites and the bulk air. Rewriting the equation expressing water concentration as vapour pressure, the soil resistance can be calculated by measuring E as the rate of evaporation from a lysimeter following the method of Daamen et al. (1993). Results both for bare soil and soil under the plant canopy showed an inverse relationship between soil resistance and soil water content (Fig. 3). These patterns were similar to that reported by previous studies (Shu Fen Sun, 1982; Katerji and Perrier, 1985; Wallace et al., 1986 all cited in Wallace, 1995) but they vary widely because of differences in the depths over which soil water content was measured (Wallace, 1995).

During the course of the experiment, the gravimetric water content of the soil (θ) under shrub was higher than the gravimetric water content of bare soil. Although there are not enough experimental points to fully determine the curves for the whole range of soil water content, the data suggest that the soil under the canopy behaves differently from that in the open, since higher resistances are found for the substrate under the canopy when compared to that in the open under wetter conditions. One of the possible reasons for this is the different nature of the substrate under the canopy of the *R. sphaerocarpa* where the ground is covered by a matt of leaf litter and patches of annuals. The combination of these substrate elements appear to increase the resistance to water loss under the canopy relative to the bare soil in the open. On average evaporation from the substrate under shrub was 60.5% ± 7.1% less than if it had not had the protection of annuals and litterfall. The equations between soil resistance and soil water content (gravimetric content, kg kg^{-1}) for bare soil (r_s^{bs}) and soil under *R. sphaero-*

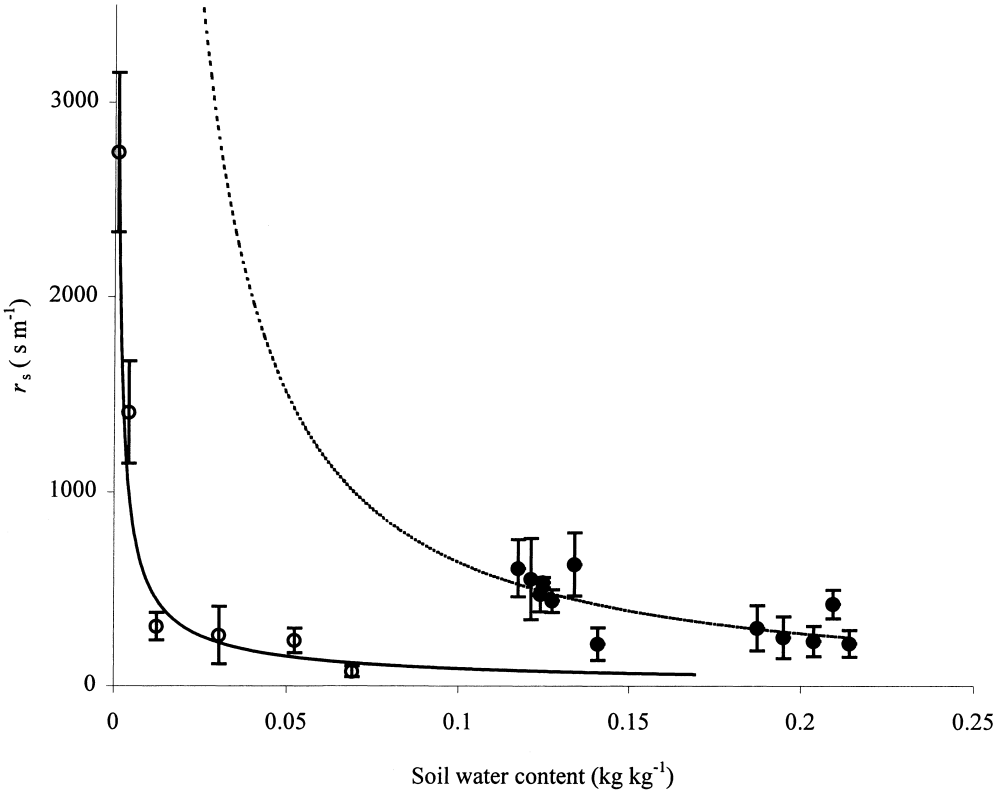

Fig. 3. Relationships between soil resistance for bare soil r_s^{bs} (○) and soil under plant r_s^{s} (●) vs. soil water content θ. Each point is the daily averaging of 20 min data during the period, 25 April to 4 May. The lines are fitted curves of the form $r = a\theta^{b}$. Points are ±1 standard error.

carpa canopy (r_s^{s}) were used in the evapotranspiration model.

$$r_s^{bs} = 15.4\theta^{-0.76}, \quad (r^2 = 0.92,\ n = 6) \qquad (18)$$

$$r_s^{s} = 37.5\theta^{-1.23}, \quad (r^2 = 0.53,\ n = 12) \qquad (19)$$

4.2. Comparison of predictions of the evapotranspiration model with field measurements

Evaporation rates (20 min) predicted by the 'original' model in general underestimated rates measured using the Bowen Ratio energy balance system (Fig. 4). The predictions from the model described in the present study which includes improved parameterisation of soil evaporation, soil aerodynamic conductance and the modified energy balance gave estimates much closer to those measured by the Bowen Ratio system.

The 'original' model underestimated total daily evapotranspiration measured by Bowen Ratio energy balance method by around 21% (Table 1), while the 'modified' model overestimated evaporation by an average of 9%. The soil aerodynamic resistance and the radiation balance modification produced little improvement in the predictions of evaporation (Table 1). However, modifying the soil surface resistance produced an average overestimation of just 5%. Since the error in Bowen Ratio evapotranspiration measurements was in the order of around 7%, it is was not possible to determine whether modifying the soil surface resistance only would produced a better result than including all three modifications.

The model enables us to attribute evaporation rates to each source (shrub, soil under shrub and bare soil) (Fig. 5). These data indicate a higher evaporation rates (around 27%) from bare soil than from the plant canopies because of the larger surface area occupied

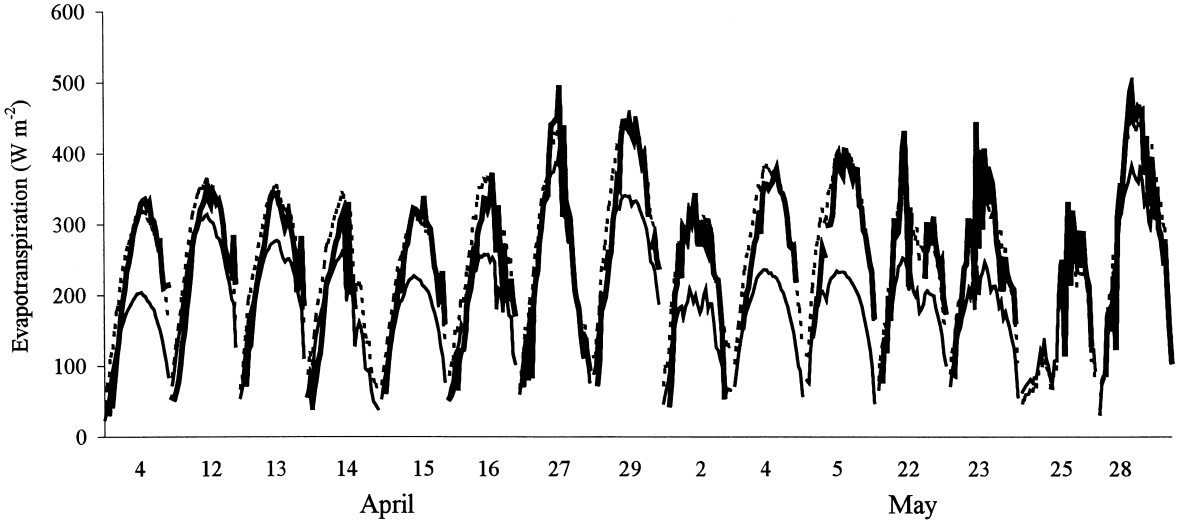

Fig. 4. Evapotranspiration measured every 20 min by Bowen Ratio energy balance system (solid line), estimated by the 'original' model (Brenner and Incoll, 1997) (thinned line), and estimated by the 'modified' model (dashed line).

by bare soil. On a unit area basis evaporation from *R. sphaerocarpa* was around 31% higher than bare soil. Evaporation from the substrate under the shrub was small, only 1.8% the rate from bare soil and 2.4% of the rate from the *R. Sphaerocarpa* canopy. Daily evaporation rates from *R. sphaerocarpa* were relatively constant over the measurement period despite high variations in the upper soil water content (0–0.25 m).

Brenner and Incoll (1997) obtained good agreement between plant evaporation predicted by the 'original' model and calculated plant evaporation rates, based on

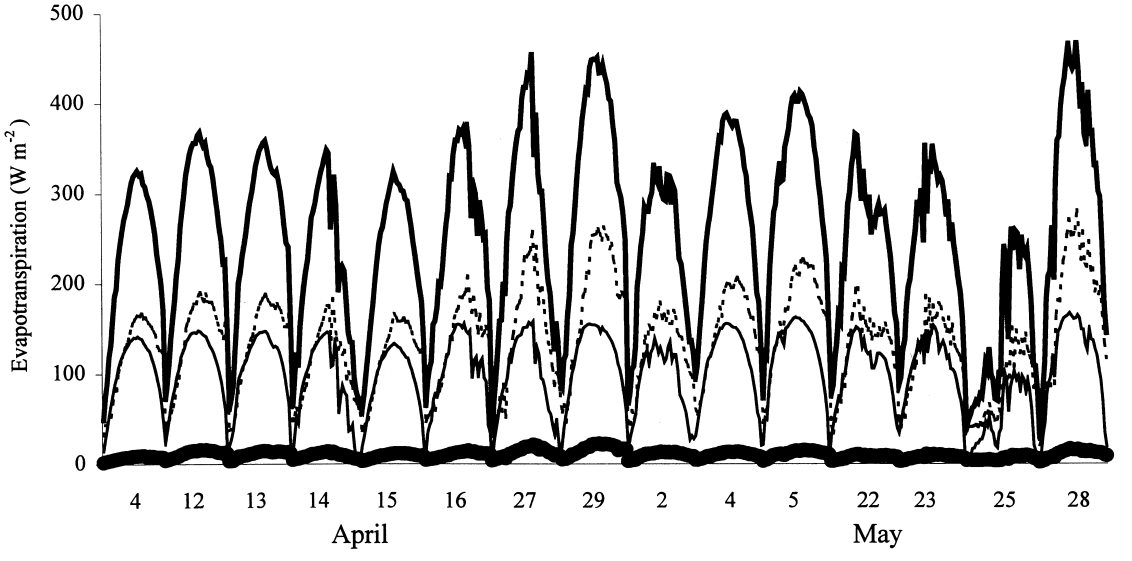

Fig. 5. Predicted evaporation rates from 'modified' model for whole surface (dashed line), plant (thinner line), bare soil (dashed line) and soil under plant (thick line).

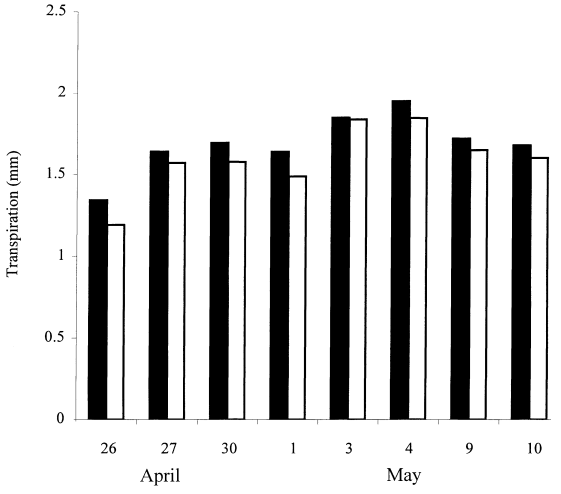

Fig. 6. Predicted total daily plant evaporation (white column) and measured plant sapflow (black column).

measurements in the field of leaf temperature, leaf conductance and meteorological conditions. In the present study good agreement was found between daily plant evaporation predicted by the model and daily sap flow measurements (Fig. 6).

Sixteen sap flow gauges were used to scale up to an entire stand using the method of Hatton et al. (1990) who found that stand transpiration could be estimated by scaling-up individual transpiration on the basis of the ground area occupied by individual plants for a thinned forest plantation where variation in tree size is low but spacing between plants is not uniform. Allen and Grime (1995), Soegaard and Boegh (1995) and Vertessy et al. (1995) recommended extrapolation of transpiration rates to unit area of land on the basis of surveys of tree size or measurements of leaf area index. A sample size of 10–12 should be sufficient for estimating the average sap flow rate with a confidence interval between 7% and 22% in monospecific, even-age stands, thus giving a good approximation for the *R. sphaerocarpa* plot of this study, (Cohen, 1991; Diawara et al., 1991; Cermak et al., 1995; Köstner et al., 1996; Loustau et al., 1996).

Daily measurements of sapflow rates were used to reduce differences produced by the capacitances that exist within the plant (Hunt et al., 1991).

The cumulative evaporation of each component was calculated over the study period that followed a dry–wet–dry soil water content cycle (Fig. 7). During this period, 83 mm of rainfall was recorded, while total accumulated evapotranspiration measured by Bowen Ratio and predicted by the model were practically the same, 161 and 160 mm, respectively. Total accumulated evapotranspiration consisted of 83 mm evaporating from bare soil, equal to the total rainfall measured. This, suggests that the rain falling on bare soil evaporated rather than drained. This observation is supported by the low measured soil surface resistance found for a wide range of soil water contents (Fig. 3). These data also indicated that the total evaporation from the *R. sphaerocarpa* stand was much (ca. 76 mm) higher than the volume of rainfall recorded over the experimental period, suggesting that *R. sphaerocarpa* can access water from sources other than the rainfall. Under the conditions here, the other source of water is stored in the deep soil horizons. The access to deep water reserves enabled the *R. sphaerocarpa* to maintain steady plant evaporation rates despite varying soil surface water conditions.

These results support previous observations made on the same species in the Rambla Honda where the deep root system of *R. sphaerocarpa* has been shown to penetrate to depths of >25 m (Haase et al., 1996a). Since evaporation from this vegetated surface exceeded rainfall over the period of study, extraction of water from deep soil layers is essential for the survival of this type of vegetation in its present vigorous form.

Physiological research on *R. sphaerocarpa* has shown it to have a very open canopy (Domingo et al., 1996, 1997, 1998) and an extensive root system (Haase et al., 1996a), suggesting a less of a conservative strategy of water use and a more of a foraging strategy for water with a large investment of resources to maintain a deep root system. It has also been found that *R. sphaerocarpa* optimises its canopy structure to drain a high proportion of effective rainfall as stemflow and has a low rainfall interception rate (Domingo et al., 1998). These adaptations play an important role in directing rainfall to deeper soil layers adjacent to the plant roots that would help to increase deep soil water storage. The low evaporation rates found below the canopy also suggest a mechanism for reducing the loss of soil water once it has been drained off the canopy after rainfall.

Our results suggest that the *R. sphaerocarpa* stand uses more water than falls directly over its area, hence

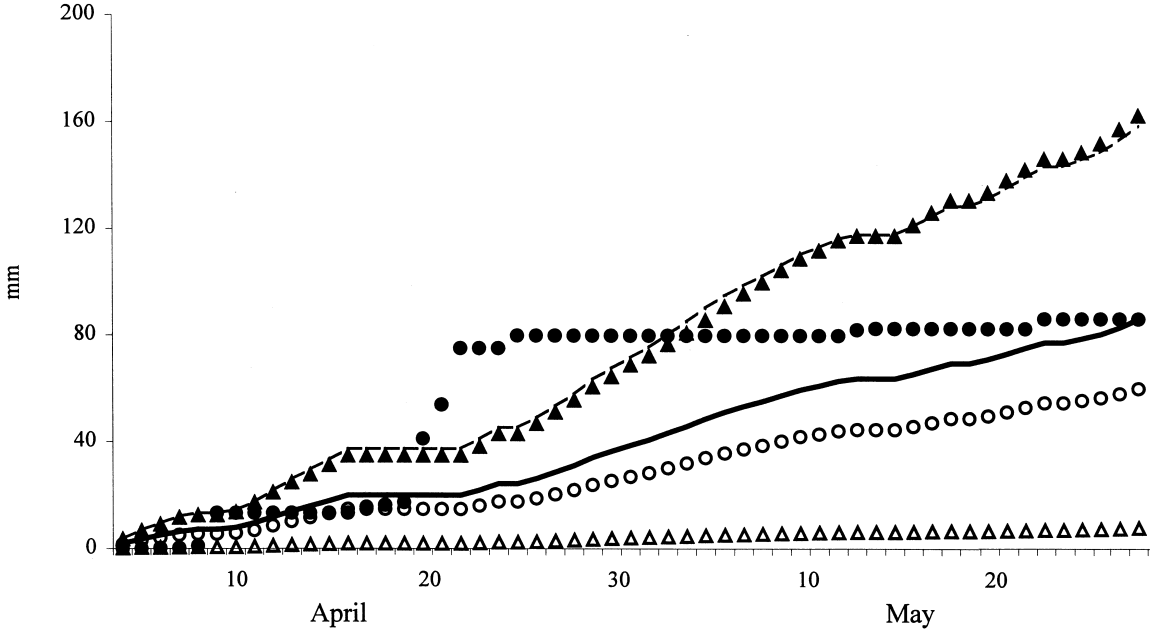

Fig. 7. Measured (▲) and modelled (– · –) evaporation from a *R. sphaerocarpa* stand, with the partition of evaporation into bare soil (solid line), substrate under shrub (△) and plant (○). Accumulated rainfall is given by (●). The soil water content of the surface soil layer underwent a dry–wet–dry cycle during the period of measurement.

it is using water that may enter the subsoil via large rain events or via subsurface flow from the surrounding catchments. The important processes in recharging these reserves of groundwater are the water redistribution by a combination of overland flow (on upper slopes covered with grass — *Stipa tenacissima*) and subsurface flow (through sandy alluvial fans) from the footslopes to the valley bottom (Puigdefábregas et al., 1998). This reinforces the hypothesis raised also for other types of vegetation that water resources redistribution processes are essential for their survival in semiarid climates i.e. stripped vegetation patterns — tiger bush — in the Sahel in Niger (Culf et al., 1993), clumped shrubs in the Chihuahuan desert in Mexico (Cornet et al., 1988), fallow savannah (Gash et al., 1991) or *S. tenacissima* grass (Puigdefábregas and Sanchez, 1996).

4.3. Sensitivity analysis of the evapotranspiration model to the modifications

A study of the sensitivity of the model to the modifications introduced in the available energy term and the surface/aerodynamic resistance terms can be summed up as follows:

The model was run with and without the modified energy balance calculation (described in the theory section). This had very little impact on predicted evapotranspiration (±1% for the whole range of values of net radiation).

The model was run substituting the relationships between soil aerodynamic resistance and wind speed between that for bare soil and soil under the plant, and vice-versa. The impact on predicted evaporation was small (<1%). Varying the albedo for bare soil by 50% and emissivity for bare soil by 4% and for plant by 2% (Table 3) resulted in a negligible change in evaporation. Varying leaf area index for the plot from 0.75, 20% and 40% higher and lower (Table 3) gave an error in evaporation rates of around ±5% and ±10%, respectively. Varying the extinction coefficient (κ) from 0.35 to 0.5 and 0.6 which may be more appropriate for net radiation produced differences of around 2% (Table 3). This low error for high variations of (κ) is an important result since the measured value of κ of 0.35 was calculated from measurements by the

Table 3
Analysis of sensitivity of model to changes in albedo, emissivity, leaf area index and extinction coefficient. The table contains the maximum, minimum, average and standard deviations ($n = 475$) of differences between the predicted evapotranspiration with the measured values of parameters and altered values

	Actual measured values	Tested values	Maximum difference (%)	Minimum difference (%)	Mean difference (%)	SD of difference (%)
Albedo (α_{bs}) (bare soil)	0.20	0.24	0.93	−1.17	−0.06	0.33
		0.17	0.78	−0.63	0.04	0.22
		0.10	2.60	−2.10	0.15	0.74
Emissivity (ε_p) (plant)	0.96	0.98	0.00	0.00	0.00	0.00
		0.94	0.00	0.00	0.00	0.00
Emissivity (ε_{bs}) (bare soil)	0.94	0.98	0.010	−0.004	2.9×10^{-5}	7×10^{-4}
		0.90	0.002	−0.006	-7×10^{-6}	2.7×10^{-4}
Leaf area index (L)	0.75	0.45	21.7	−1.6	11.8	4.0
		0.60	10.3	−0.7	5.5	1.9
		0.90	0.6	−9.2	−4.8	1.8
		1.05	1.2	−17.5	−9.0	3.4
Extintion coefficient (κ)	0.35	0.2	12.2	−1.7	4.8	2.0
		0.5	1.2	−6.6	−1.7	1.1
		0.6	1.8	−9.0	−2.0	1.6

DEMON for wavelengths <380 nm and may well differ from a κ for net radiation.

A 2% variation in the soil water content produced a change in predicted evaporation rates that increased as the soil water content decreased (Fig. 8). Results show that an error of 2% in the fractional soil water content measurement could produce an error up to 30% in predicted evapotranspiration rates when the soil water

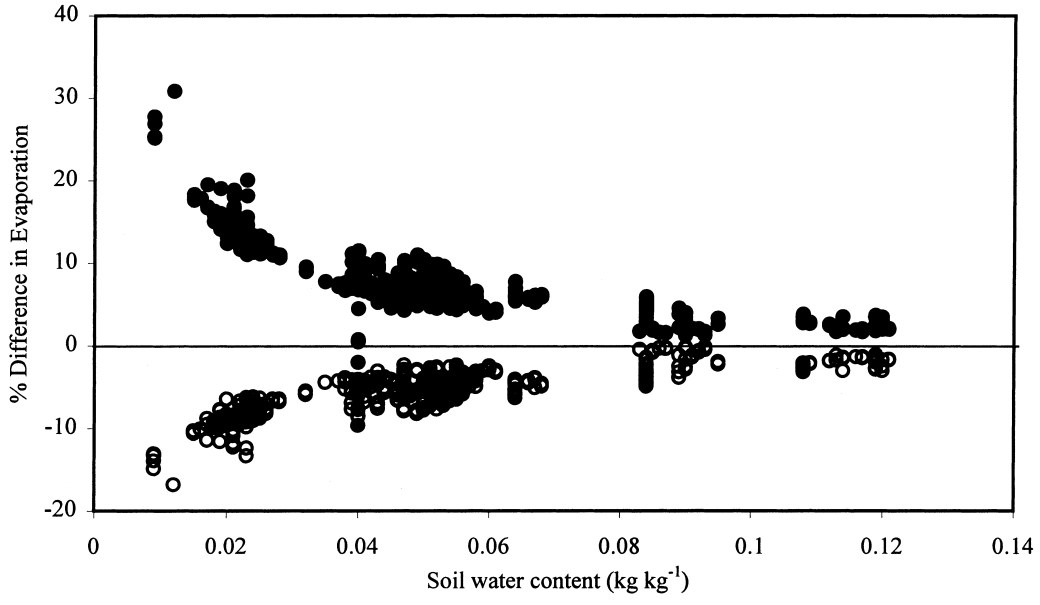

Fig. 8. Differences between predicted evaporation rates using measured soil water content and predicted evaporation rates using measured soil water content +0.02 (○) and −0.02 (●) plotted against measured soil water content.

content was low (1%) but only an error of 3% in the modelled evapotranspiration when the soil water content was 10% or higher.

5. Conclusions

Modifications made to the 'original' Brenner and Incoll (1997) model led to good agreement between predicted evapotranspiration rates and those measured by the Bowen Ratio energy balance method. This improvement was mainly achieved through improved parameterisation of the soil evaporation part of the model, achieved by relating the soil surface conductance to surface soil water content, and separating the conductance of the soil surface under the shrub from that in the open. The sensitivity analysis showed that accurate specification of soil water content is fundamental for achieving accurate predictions of evaporation in this type of environment. The more detailed specification of the radiation balance and soil aerodynamic terms by themselves did not lead to significantly better predictions by the model under the conditions found here.

A second important result, gained from the sensitivity analysis, was that errors in some variables such as albedo or κ introduced relatively small errors in predicted evaporation whereas errors in others such as soil water content could introduced large errors in such evaporation. The insensitivity of the model to improved calculation of net radiation, for our specific vegetative cover fraction (f), reflection coefficients and emissivities, which produced low values of δ, lead to little improvement in the calculation of net radiation but in other situations this may not be true.

The insensitivity of the model to the soil aerodynamic resistance term is linked to its lower quantitative importance compared to the soil surface resistances (compare Figs. 2 and 3). The advantage of the experimental method applied here is that it helps to understand the spatial variation of aerodynamic resistances for heat and mass transfer between the atmosphere and substrate in sparse vegetation. This experiment showed that there were significant differences between the environmental conditions for bare soil and soil under the plant because of the effect of annuals and litter under the *R. sphaerocarpa* canopy. This paper also proposes a simple formulation for calculating soil aerodynamic resistances based on wind speed in evapotranspiration modelling. Although this approach is empirical and linked to a specific value of f, it should prove to be useful further research will enable a more generally applicable formula to be applied to areas with different values of f.

The estimation of evaporation and its partition supports previous observations that *R. sphaerocarpa* is able to access deep reserves of water stored in the soil. Since evaporation from this vegetated surface exceeded rainfall over the period of study, extraction of water from deep soil layers appears to be essential for the survival of this type of vegetation in its present vigorous form. These results support the conclusions of other studies on physiological aspects of the same species permitting to conclude that *R. sphaerocarpa* has a strategy for foraging for water with a large investment of resources to maintain a deep root system, rather than conserving water use.

Our results also demonstrate that the *R. sphaerocarpa* stand can evaporate more water than the precipitation that falls over its geographical extent, hence it is using water that may enter the subsoil via large rain events or via subsurface flow from the surrounding catchments. Reforestation of the slopes of these catchments with conifers is likely to contribute to a decrease the magnitude, and frequency of groundwater recharge that would, amongst other consequences, threaten the existence of plants like *R. sphaerocarpa* dependant on deep groundwater reserves.

Acknowledgements

This work has been funded by a postdoctoral contract of the Ministerio de Educación y Cultura of Spain for the first author, by a predoctoral grant of the Ministerio de Educación y Cultura of Spain for the second author, by the MEDALUS III project (Mediterranean Desertification and Land Use) funded by the European Community under its Environment Programme contract number EV5V CT92-0164 and by the Spanish project funded by the CICYT (ref. CLI95-1874). We would like to thank Dr. Matthias Boer and anonymous referees for their helpful and constructive comments on the manuscript. Miguel Angel Domene is thanked for indispensable technical assistance during field measurements.

References

Allen, S.J., Grime, V.L., 1995. Measurements of transpiration from savannah shrubs using sap flow gauges. Agric. For. Meteorol. 75, 23–41.

Brenner, A.J., Cueto, M., García, J., Gilabert, M.A., Incoll, L.D., Martínez, J., Porter, E., Pugnaire, F.I., Younis, M.T., 1995. A comparison of direct and indirect methods for measuring leaf and surface area of individual Retama bushes. Plant, Cell and Environ. 18, 1332–1340.

Brenner, A.J., Incoll, L.D., 1997. The effect of clumping and stomatal response on evaporation from sparsely vegetated shrublands. Agric. For. Meteorol. 84, 187–205.

Cermak, J., Cienciala, E., Kucera, J., Lindroth, A., Bednarova, E., 1995. Individual variation of sap-flow rate in large pine and spruce trees and stand transpiration: a pilot study at the central NOPEX site. J. Hydrol. 168, 17–27.

Choudhury, B.J., Monteith, J.L., 1988. A four-layer model for the heat budget of homogenous land surfaces. Quart. J. Royal Meteorol. Soc. 114, 373–398.

Cohen, Y., 1991. Determination of orchard water requirement by a combined trunk sap flow and meteorological approach. Irrig. Sci. 12, 93–98.

Cornet, A.P., Delhoume, J.P., Montana, C., 1988. Dynamics of striped vegetation patterns and water balance in the Chihuahuan desert. In: During, H.J., Werger, M.J.A., Willems, J.H. (Eds.), Diversity and Pattern in Plant Communities. SPB Academic Publishing, The Hague, Netherlands, pp. 221–231.

Culf, A.D., Allen, S.J., Gash, J.H.C., Lloyd, C.R., Wallace, J.S., 1993. Energy and water budgets of an area of patterned woodland in the Sahel. Agric. For. Meteorol. 66, 65–80.

Daamen, C.C., Simmonds, L.P., Wallace, J.S., Laryea, K.B., Sivakumar, M.V.K., 1993. Use of microlysimeters to measure evaporation from sandy soils. Agric. For. Meteorol. 65, 159–173.

Diawara, A., Lousteau, D., Berbigier, P., 1991. Comparison of two methods for estimating the evaporation of a *Pinus pinaster* (Ait.) stand: sap flow and energy balance with sensible heat flux measurements by an eddy covariance method. Agric. For. Meteorol. 54, 49–66.

Dolman, A.J., 1993. A multiple-source land surface energy balance model for use in general circulation models. Agric. For. Meteorol. 65, 21–45.

Domingo, F., van Gardingen, P.G., Brenner, A.J., 1996. Leaf boundary layer conductance of two native species in south-east Spain. Agric. For. Meteorol. 81(3/4), 179–199.

Domingo, F., Moro, M.J., Sanchez, G., Brenner, A.J., van Gardingen, P.R., 1997. Leaf and canopy boundary layer conductances of two semi-arid species (*Retama sphaerocarpa* (L.) Boiss and *Stipa tenacissima* L.). Mediterránea Ser. Biol. 16, 37–43.

Domingo, F., Sánchez, G., Moro, M.J., Brenner, A.J., Puigdefábregas, J., 1998. Measurement and modelling of rainfall interception by three semi-arid canopies. Agric. For. Meteorol. 91, 275–292.

Domingo, F., Villagarcía, L., Brenner, A.J., Puigdefábregas, J., 1999. Radiation balance of a semiarid *Retama sphaerocarpa* shrubland (internal revision).

Gash, J.H.C., Wallace, J.S., Lloyd, C.R., Dolman, A.J., Sivakumar, M.V.K., Renard, C., 1991. Measurements of evaporation from fallow Sahelian savannah at the start of the dry season. Quart. J. Royal Meteorol. Soc. 117, 749–760.

Gurney, R.J., Sewell, I.J., 1997. Observation and simulation of energy budgets at the surface of a prairie grassland. In: van Gardingen, P.R., Foody, G.M., Curran, P.J. (Eds.), Scaling-up: From Cell to Landscape, Society for Experimental Biology, Seminar Series: 63, Cambridge University Press, Cambridge, UK, pp. 319–346.

Haase, P., Pugnaire, F.I., Fernández, E.M., Puigdefábregas, J., Clark, S.C., Incoll, L.D., 1996a. An investigation of rooting depth of the semiarid shrub *Retama sphaerocarpa* (L.) Boiss. by labelling of ground water with a chemical tracer. J. Hydrol. 177, 23–31.

Haase, P., Pugnaire, F.I., Clark, S.C., Incoll, L.D., 1996b. Spatial patterns in two-tiered semi-arid shrubland in southeastern Spain. J. Vegetation Sci. 7, 527–534.

Hatton, T.J., Catchpole, E.A., Vertessy, R.A., 1990. Integration of sapflow velocity to estimate plant water use. Tree Physiol. 6, 201–209.

Hunt, R.E., Running, S.R., Federer, C.A., 1991. Extrapolating plant water flow resistances and capacitances to regional scales. Agric. For. Meteorol. 54, 169–195.

Jones, H.G., 1992. Plants and Microclimate. Cambridge University Press. Cambridge, UK, 428 pp.

Kays, W.M., Crawford, M.E., 1980. Convective Heat and Mass Transfer. MacGraw-Hill, New York. 420 pp.

Köstner, B., Biron, P., Siegwolf, R., Granier, A., 1996. Estimates of water vapour flux and canopy conductance of Scots Pine at the tree level utilizing different xylem sap flow methods. Theor. Appl. Climatol. 53, 105–113.

Loustau, D., Berbigier, P., Roumagnac, P., Arruda-Pacheco, C., David, S., Ferreira, M., Perreira, J., Tavares, R., 1996. Transpiration of 64-year-old maritime pine stand in Portugal I. Seasonal course of water flux through maritime Pine. Oecologia 107, 33–42.

Lowe, P.R., 1976. An approximating polynomial for computation of saturation vapour pessure. J. Appl. Meteorol. 16, 100–103.

McInnes, K.J., Heilman, J.L., Savage, M.J., 1994. Aerodynamic conductances along a bare ridge-furrow tilled soil surface. Agric. For. Meteorol. 68, 119–131.

McInnes, K.J., Heilman, J.L., Lascano, R.J., 1996. Aerodynamic conductances at the soil surface in a vineyard. Agric. For. Meteorol. 79, 29–37.

Monteith, J.L., 1965. Evaporation and the environment. Proc. Soc. Exp. Biol. 19, 205–234.

Nichols, W.D., 1992. Energy budgets and resistances to energy transport in sparsely vegetated rangeland. Agric. For. Meteorol. 60, 221–247.

Nie, D., Flitcroft, I.D., Kanemasu, E.T., 1992. Performance of Bowen Ratio systems on a slope. Agric. For. Meteorol. 59, 165–181.

Puigdefábregas, J., Sanchez, G., 1996. Geomorphological implications of vegetation patchiness in semiarid slopes. In: Anderson, M., Brooks, S. (Eds.), Advances in Hillslope Processes, Wiley, New York, Chap. 2, pp. 1028–1060.

Puigdefábregas, J., Aguilera, C., Alonso, J.M., Brenner, A.J., Clark, S.C., Cueto, M., Delgado, L., Domingo, F., Gutiérrez, L., Incoll, L.D., Lázaro, R., Nicolau, J.M., Sánchez, G., Solé, A., Vidal, S., 1996. The Rambla Honda field site. Interactions of soil and vegetation along a catena in semi-arid SE Spain. In: Brandt, J., Thornes, J.B. (Eds.), Mediterranean Desertification and Land Use, Wiley, London, pp. 137–168.

Puigdefábregas, J., del Barrio, G., Boer, M., Gutierrez, L., Solé, A., 1998. Differential responses of hillslope and channel elements to rainfall events in a semi-arid area. Geomorphology 23, 337–351.

Rouse, W.R., Carlson, D.W., Weick, E.J., 1992. Impacts of summer warming on the energy and water balance of wetland tundra. Climate Change 22, 305–326.

Shuttleworth, W.J., Wallace, J.S., 1985. Evaporation from sparse crops-an energy combination theory. Quart. J. Royal Meteorol. Soc. 111, 839–855.

Shuttleworth, W.J., Gurney, R.J., 1990. The theoretical relationship between foliage temperature and canopy resistance in sparse crops. Quart. J. Royal Meteorol. Soc. 116, 498–519.

Soegaard, H., Boegh, E., 1995. Estimation of evapotranspiration from a millet crop in the Sahel combining sap flow, leaf area index and eddy correlation technique. J. Hydrol. 116, 265–282.

Vertessy, R.A., Benyon, R.G., Osullivan, S.K., Gribben, P.R., 1995. Relationships between stem diameter, sapwood area, leaf area and transpiration in a young mountain ash forest. Tree Physiol. 15, 559–567.

Vidal, S., 1994. A device for simultaneous measurement of soil moisture and electrical conductivity. Patent No. 9401681.

Vidal, S., Domene, M.A., Domingo, F., Solé, A., Puigdefábregas, J., 1996. Desarrollo y calibración de un nuevo sensor de humedad del suelo. In: Instituto Tecnológico Geominero de España (Ed.), Proc. 4th Simposio sobre el agua en Andalucia, vol I, pp. 101–111.

Wallace, J.S., 1995. Calculating evaporation: resistance to factors. Agric. For. Meteorol. 73, 353–366.